

Low-Cost Flexible Nano-Sulfide/Carbon Composite Counter Electrode for Quantum-Dot-Sensitized Solar Cell

Minghui Deng · Quanxin Zhang · Shuqing Huang ·
Dongmei Li · Yanhong Luo · Qing Shen · Taro Toyoda ·
Qingbo Meng

Received: 1 March 2010 / Accepted: 27 March 2010 / Published online: 14 April 2010
© The Author(s) 2010. This article is published with open access at Springerlink.com

Abstract Cu₂S nanocrystal particles were in situ deposited on graphite paper to prepare nano-sulfide/carbon composite counter electrode for CdS/CdSe quantum-dot-sensitized solar cell (QDSC). By optimization of deposition time, photovoltaic conversion efficiency up to 3.08% was obtained. In the meantime, this composite counter electrode was superior to the commonly used Pt, Au and carbon counter electrodes. Electrochemical impedance spectra further confirmed that low charge transfer resistance at counter electrode/electrolyte interface was responsible for this, implied the potential application of this composite counter electrode in high-efficiency QDSC.

Keywords Quantum dot · Sensitized solar cell · Composite · Flexible · Carbon electrode · Cu₂S · CdS/CdSe

Introduction

The quantum-dot-sensitized solar cell has aroused great research interests due to the superior properties of

semiconductor quantum dots (QDs) in recent years [1–11]. The merits of QDs include higher extinction coefficient in visible light spectrum [1], multiple excitons generation through impact ionization [2] and readily tuned bandgap by size control [6]. Therefore, various semiconductor QD sensitizers, such as CdS [1, 4, 5], CdSe [6, 7], CdTe [8], InAs [9], InP [10], and their linking to the photoanode [12–14] have been widely studied for QDSCs. Meanwhile, as another important part of the sandwich-type QDSC, more attention was also paid to the research of counter electrode (CE) lately [14–16]. Bisquert et al. [14] found that Pt CE constituted a limiting factor for the cell performance because the sulfides (S²⁻, S_x²⁻ ions) can adsorb onto Pt surface and impair its electrocatalytic activity. Lee et al. [15] verified this result and proved that Au CE was more immune to the sulfur ions with high energy conversion efficiency up to 4.22% for CdS/CdSe QDSC.

As we know, for all kinds of solar cells, the cost reduction is crucial for their future development all the time. Two typical strategies in cost cutting include the introduction of (a) easily handled preparation methods and (b) inexpensive alternative materials into the fabrication of solar cells, such as low-cost electrochemical etching method to prepare silicon nanocrystallites [17] and various conducting polymers [18, 19] or carbon materials [20, 21]. In dye-sensitized solar cells (DSCs), as promising low-cost replacements of Pt CE, carbon CEs have been widely investigated [20–27]. For QDSCs, latest research revealed that carbon electrode exhibited much higher activity beyond Pt in polysulfide redox system (S²⁻/S_x²⁻) and the cell efficiency of 1.47% was obtained [16]. Another cheap material Cu₂S also exhibited possible application as CE for QDSCs in virtue of its high electrocatalytic activity reported by Hodes et al. [28]. A newly published result showed that with the CE of Cu₂S made from brass in CdSe

M. Deng · Q. Zhang · S. Huang · D. Li · Y. Luo ·
Q. Meng (✉)
Beijing National Laboratory for Condensed Matter Physics,
Institute of Physics, Chinese Academy of Sciences,
100190 Beijing, China
e-mail: qbmeng@aphy.iphy.ac.cn

Q. Shen · T. Toyoda
Department of Applied Physics and Chemistry, The University
of Electro-Communications, 1-5-1 Chofugaoka, Chofu, Tokyo
182-8585, Japan

Q. Shen
PRESTO, Japan Science and Technology Agency, 4-1-8 Honcho
Kawaguchi, Saitama 332-0012, Japan

QDSC, the fill factor (FF) was increased remarkably and photovoltaic efficiency was improved to 1.83% [7]. Here, in order to further increase the cell efficiency, conductive graphite with noticeable activity was associated with the highly active Cu_2S by the in situ deposition of Cu_2S nanoparticles on flexible graphite paper. This nano-sulfide/carbon composite electrode was introduced into CdS/CdSe QDSC for the first time and superior energy conversion efficiency of 3.08% was achieved.

Experimental

Preparation of Counter Electrode

The flexible graphite paper used as conductive substrate was the same as our previous research [25]. In order to increase the functionalized sites for Cu_2S adhesion on the surface of graphite, the substrate was annealed under 450 °C for 30 min in the air before use. Solvent thermal method was employed to deposit Cu_2S nanoparticles. The procedures were described as follows [29]: 20 mM $Cu(CH_3COO)_2$ and 10 mM thiourea were dissolved in diethylene glycol (DEG) sequentially and transferred to Teflon autoclave. Then, the annealed graphite paper was immersed and the autoclave was sealed and maintained at 180 °C for 2–12 h. After the reaction, the treated graphite was washed with deionized water three times and dried at 60 °C under vacuum overnight to get rid of water and residual DEG. This kind of CE was referred as nano- Cu_2S/C in the following. For comparison, the annealed graphite paper, the thermally decomposed Pt electrodes on F-doped SnO_2 conducting glass (FTO, 15 Ω/\square) and annealed graphite paper, carbon counter electrodes on these two substrates [16] as well as Au electrode on FTO glass by evaporative deposition were also used as CEs for QDSCs.

Cell Fabrication

CdS/CdSe-sensitized photoanode was fabricated by a previously published chemical bath method [30, 31]. CdS was pre-deposited onto TiO_2 nanoporous film in the aqueous solution of 20 mM $CdCl_2$, 66 mM NH_4Cl , 140 mM thiourea and 230 mM ammonia, followed by the CdSe deposition in a mixture with the composition of 80 mM sodium selenosulphate (Na_2SeSO_3 , prepared by dissolving 0.2 M Se powder in a 0.5 M Na_2SO_3 solution at 80 °C), 80 mM $CdSO_4$ and 160 mM nitrilotriacetic acid tripotassium salt (NTA, $N(CH_2COOK)_3$). Surface passivation with ZnS was realized by dipping the sensitized photoanode alternatively into 0.1 M $Zn(CH_3COO)_2$ and 0.1 M Na_2S solution for 1 min twice [7, 12]. Polysulfide electrolyte with 1 M Na_2S and 1 M S aqueous solution was used as redox agent.

Electrolytes were dropped on the sensitized photoanode, and counter electrode was clipped firmly to make a sandwich structure QDSC. A 50- μm silicone film was used as spacer. The active area of the cell was 0.15 cm^2 .

Measurements

The morphology of the nano- Cu_2S/C CE was investigated by a scanning electron microscope (SEM) (FEI, XL30 S-FEG). The X-ray diffraction (XRD, M18X-AHF, MAC Science) pattern was recorded with Cu K α radiation source for the dried powders from the reaction autoclave. The cells were irradiated by simulated AM1.5 irradiation (Oriel, 91192). Current–photovoltage (I – V) characteristics were recorded by a potentiostat (Princeton Applied Research, Model 263A). Electrochemical impedance spectroscopy (EIS) measurements were carried out on electrochemical workstations (Zahner, IM6ex) under illumination. During the measurement, the cell was biased with open-circuit voltage under sinusoidal perturbation of 10 mV with the frequency scanning range 10^{-1} – 10^5 Hz. EIS results were fitted with Z-view to obtain the charge transfer resistance (R_{ct}) at the CE/electrolyte interface.

Results and Discussion

Figure 1 illustrates the XRD pattern of the synthesized Cu_2S after 5 h solvent thermal reaction. The peaks of corresponding crystal planes were indexed in the figure, matching to the hexagonal phase chalcocite β - Cu_2S (JCPDS card no. 46-1195, $a = 3.96$ Å, $c = 6.78$ Å). The broad peak at about 30° should be ascribed to the glass sample holder [29]. According to Scherrer equation, the crystal size was estimated about 25 nm.

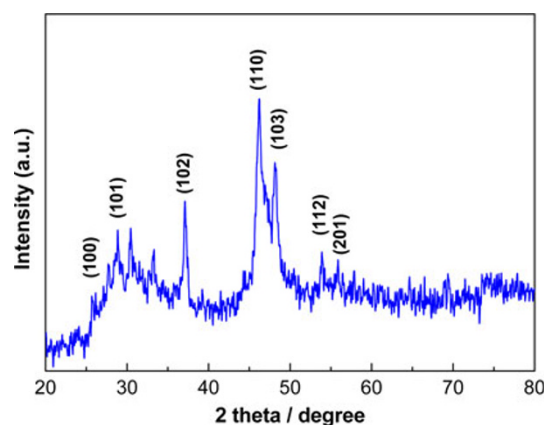


Fig. 1 XRD pattern of solvent thermal synthesized Cu_2S nanoparticles

Figure 2 shows the surface morphologies of graphite paper before and after 5 h Cu_2S deposition. Before the deposition of Cu_2S , graphite surface was clean and smooth in microscale and the layered structure was clearly visible. After the solvent thermal treatment, a great amount of Cu_2S nanocrystal particles was deposited onto the surface of graphite with spread dispersion. These grafted particles afford much larger surface area compared with the plain graphite surface, leading to obvious improvement in the number of reaction sites. Thus, these well-dispersed Cu_2S nanoparticles should be more beneficial for the reduction of S_x^{2-} ions. Moreover, the area without Cu_2S loading is not completely inert in redox reaction. As indicated below, graphite itself is capable of working as CE, although not so efficient as Cu_2S . Thus, this nano- Cu_2S /graphite composite electrode will present attractive preponderance in QDSCs.

Concerning the influence of Cu_2S deposition time on the performance of composite CEs, a series of I–V curves were shown in Fig. 3. Both the photocurrent and photovoltage increased with treating time until they reached the peak value and then decreased. Here, the optimal treating time is 5 h with the parameters of 10.68 mA cm^{-2} in photocurrent density (J_{sc}), 497 mV in open circuit voltage (V_{oc}) and

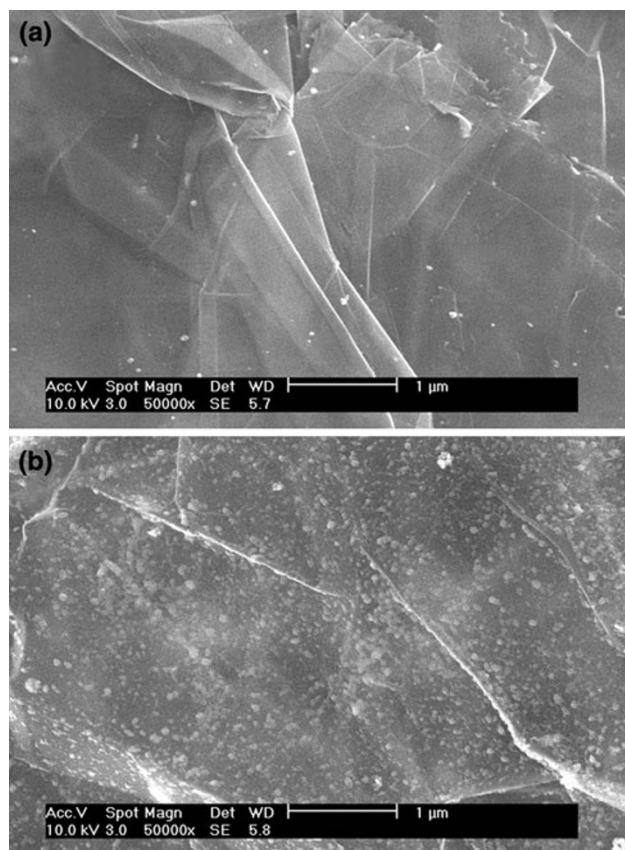


Fig. 2 SEM images of the graphite paper surface **a** before and **b** after 5 h solvent thermal treatment

0.581 in FF and photovoltaic conversion efficiency (η) up to 3.08%. In the following, all the experiments were conducted using the composite CEs with 5 h Cu_2S deposition.

QDSCs fabricated with various CEs were also tested and the results were shown in Fig. 4 (detailed data showed in Table 1). With the η of 0.66%, graphite CE revealed similar activity as the widely used thermally decomposed Pt on FTO, which has an efficiency of 0.68%. This result indicated that the low-cost flexible graphite paper was very advantageous to be used as the conductive substrate in QDSC compared with FTO ($\eta = 0.04\%$). By the combination of nanocrystal Cu_2S and graphite paper, energy conversion efficiency was significantly boosted to 3.08%, showing the all-around superiority of nano- Cu_2S /C composite CE over other counterparts. As for the Au electrode on FTO, although the J_{sc} and V_{oc} are much better than Pt on FTO, its FF is too low to promote the cell efficiency remarkably. This may be due to the small surface area of smooth Au film or the catalytic activity of evaporative deposited Au was not high enough.

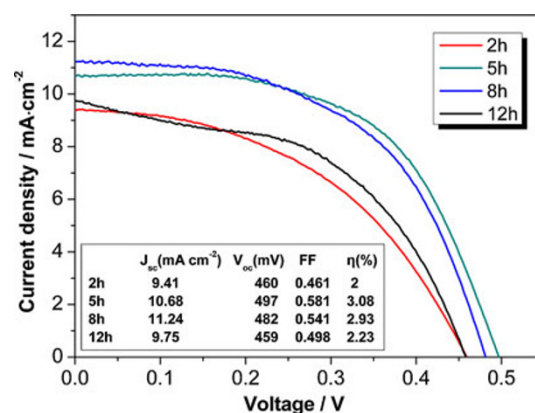


Fig. 3 I–V characteristics for QDSCs with counter electrodes of different Cu_2S deposition time (Under illumination of AM 1.5)

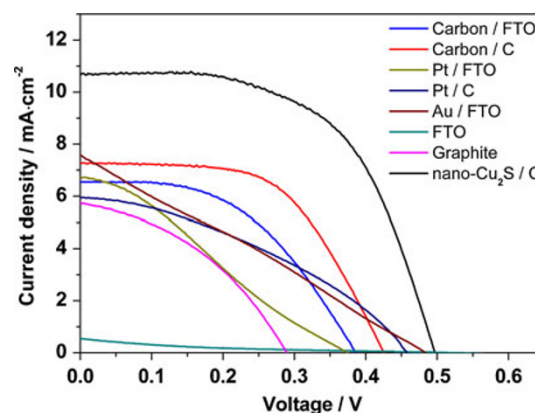


Fig. 4 I–V characteristics for QDSCs with different counter electrodes (Under illumination of AM 1.5)

Table 1 Photovoltaic parameters of tested QDSCs, together with R_{\square} and R_{ct} value of various counter electrodes

Counter electrode	J_{sc} (mA cm ⁻²)	V_{oc} (mV)	FF	η (%)	R_{\square} (Ω/\square)	R_{ct} (Ω cm ²)
Nano-Cu ₂ S/C	10.68	497	0.581	3.08	0.044	0.063
Graphite	5.75	289	0.394	0.66	0.038	0.749
Au/FTO	7.57	484	0.269	0.98	0.24	0.196
Pt/C	5.93	458	0.376	1.02	0.042	1.088
Pt/FTO	6.73	374	0.271	0.68	0.015	0.886
Carbon/C	7.25	425	0.571	1.76	0.066	0.166
Carbon/FTO	6.48	387	0.495	1.24	14.6	0.795

As we know, the S_x^{2-} reduction rate is primarily determined by the catalytic activity of counter electrodes while keeping other factors unchanged (such as photoanode, electrolyte, etc.). Here, charge transfer process at different CEs was investigated by EIS. Figure 5 illustrated the Nyquist plots of QDSCs with different CEs, where the semicircle appeared in the high-frequency region was assigned to be R_{ct} [24, 32]. From the data listed in Table 1, R_{ct} (0.063 Ω cm²) of nano-Cu₂S/C is much smaller than those of other CEs used in present case. This explains the high J_{sc} and FF of nano-Cu₂S/C in I–V test [7, 14]. Moreover, on the basis of the formula (1):

$$R_{ct} = RT/nFJ_0 \quad (1)$$

where R is the molar gas constant, T the temperature, n the number of electrons transferred in the reaction, F the Faraday constant and J_0 the exchange current density. Assuming $n = 2$ for the reaction $S_2^{2-} + 2e = 2S^{2-}$, the J_0 of 205 mA cm⁻² is obtained. This high value of J_0 means the nano-Cu₂S/C composite CE used here is dynamically

active enough to afford J_{sc} in a QDSC whose value is an order higher than the present one, completely competent for the application in high-efficiency quantum-dot-sensitized solar cells.

Conclusion

Cu₂S nanoparticles were deposited on the surface of graphite paper to obtain a composite counter electrode for CdS/CdSe-sensitized solar cell. With the cell parameters of $J_{sc} = 10.68$ mA cm⁻², $V_{oc} = 497$ mV, $FF = 0.581$ and $\eta = 3.08\%$, QDSC with nano-Cu₂S/C composite CE exhibits superior performance to the Pt, Au and carbon CEs. Electrochemical impedance spectroscopy measurement indicates that the R_{ct} at CE/electrolyte was very low and made the composite CE an excellent candidate for high-efficiency QDSCs.

Acknowledgments We gratefully acknowledge the support of the National Science Fund for Distinguished Young Scholars under Grant No. 20725311, the National Natural Science Foundation of China under Grant No. 20673141, 20703063 and 20873178, Strategic China-Japan (NSFC-JST) Joint Research Program under Grant No. 20721140647, the National Basic Research Program of China (“973”) under Grant No. 2006CB202606, the National High Technology Research and Development Program (“863”) under Grant No. 2006AA03Z341 and the 100-Talents Project of Chinese Academy of Sciences. Part of this work was supported by JST PRESTO program and by a Grant-in Aid for Scientific Research (No.21310073) from the Ministry of Education, Culture, Sports, Science and Technology of the Japanese Government.

Open Access This article is distributed under the terms of the Creative Commons Attribution Noncommercial License which permits any noncommercial use, distribution, and reproduction in any medium, provided the original author(s) and source are credited.

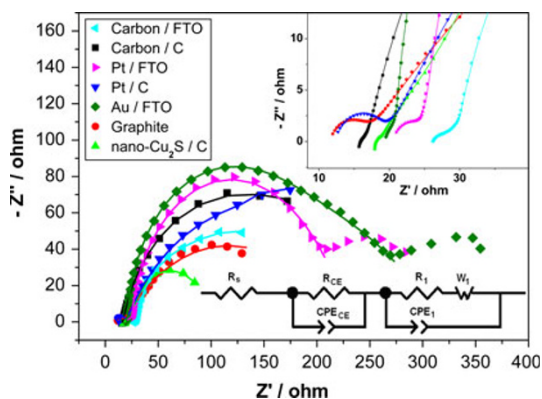


Fig. 5 Nyquist plots (scattered) and their fitting results (line) of QDSCs with various counter electrodes under bias of V_{oc} (under illumination of AM1.5). The inset (above) shows the detailed plots in the high-frequency region; (below) the equivalent circuit for the QDSC with the representation of impedance at CE/electrolyte interface (subscript CE), TiO₂/CdS/CdSe/electrolyte interface (subscript I) and series resistance (subscript s, including resistance in TiO₂ film and electrolyte). The symbols R and CPE describe a resistance and a constant phase element, respectively; W accounts for finite-length Warburg diffusion

References

1. W.W. Yu, L. Qu, W. Guo, X. Peng, Chem. Mater. **15**, 2854 (2003)
2. A.J. Nozik, Inorg. Chem. **44**, 6893 (2005)
3. Y.-L. Lee, C.-H. Chang, J. Power Sources **185**, 584 (2008)
4. S. Hotchandani, P.V. Kamat, J. Phys. Chem. **96**, 6834 (1992)

5. L.M. Peter, D.J. Riley, E.J. Tull, K.G.U. Wijayantha, *Chem. Comm.* **10**, 1030 (2002)
6. I. Robel, V. Subramanian, M. Kuno, P.V. Kamat, *J. Am. Chem. Soc.* **128**, 2385 (2006)
7. S. Giménez, I. Mora-Seró, L. Macor, N. Guijarro, T. Lana-Villarreal, R. Gómez, L.J. Diguna, Q. Shen, T. Toyoda, J. Bisquert, *Nanotechnology* **20**, 295204 (2009)
8. K. Ernst, R. Engelhardt, K. Ellmer, C. Kelch, H.-J. Muffler, M.-Ch. Lux-Steiner, R. Könenkamp, *Thin Solid Films* **387**, 26 (2001)
9. P. Yu, K. Zhu, A.G. Norman, S. Ferrere, A.J. Frank, A.J. Nozik, *J. Phys. Chem. B* **110**, 25451 (2006)
10. A. Zaban, O.I. Mičić, B.A. Gregg, A.J. Nozik, *Langmuir* **14**, 3153 (1998)
11. K. Yu, J. Chen, *Nanoscale Res. Lett.* **4**, 1 (2009)
12. L.J. Diguna, Q. Shen, J. Kobayashi, T. Toyoda, *Appl. Phys. Lett.* **91**, 023116 (2007)
13. K.S. Leschkies, R. Divakar, J. Basu, E. Enache-Pommer, J.E. Boercker, C.B. Carter, U.R. Kortshagen, D.J. Norris, E.S. Aydil, *Nano Lett.* **7**, 1793 (2007)
14. I. Mora-Seró, S. Giménez, T. Moehl, F. Fabregat-Santiago, T. Lana-Villareal, R. Gómez, J. Bisquert, *Nanotechnology* **19**, 424007 (2008)
15. Y.-L. Lee, Y.-S. Lo, *Adv. Funct. Mater.* **19**, 604 (2009)
16. Q. Zhang, Y. Zhang, S. Huang, X. Huang, Y. Luo, Q. Meng, D. Li, *Electrochem. Commun.* **12**, 327 (2010)
17. V. Švrček, *Nano-Micro Lett.* **1**, 40 (2009)
18. K.M. Coakley, M.D. McGehee, *Chem. Mater.* **16**, 4533 (2004)
19. Z. Li, B. Ye, X. Hu, X. Ma, X. Zhang, Y. Deng, *Electrochem. Commun.* **11**, 1768 (2009)
20. A. Kay, M. Grätzel, *Sol. Energy Mater. Sol. Cells* **44**, 99 (1996)
21. N. Papageorgiou, *Coord. Chem. Rev.* **248**, 1421 (2004)
22. K. Imoto, K. Takahashi, T. Yamaguchi, T. Komura, J. Nakamura, K. Murata, *Sol. Energy Mater. Sol. Cells* **79**, 459 (2003)
23. K. Suzuki, M. Yamaguchi, M. Kumagai, S. Yanagida, *Chem. Lett.* **32**, 28 (2003)
24. K. Li, Y. Luo, Z. Yu, M. Deng, D. Li, Q. Meng, *Electrochem. Commun.* **11**, 1346 (2009)
25. J. Chen, K. Li, Y. Luo, X. Guo, D. Li, M. Deng, S. Huang, Q. Meng, *Carbon* **47**, 2704 (2009)
26. H. Lindström, A. Holmberg, E. Magnusson, S.-E. Lindquist, L. Malmqvist, A. Hagfeldt, *Nano Lett.* **1**, 97 (2001)
27. T.N. Murakami, S. Ito, Q. Wang, M.K. Nazeeruddin, T. Bessho, I. Cesar, P. Liska, R. Humphry-Baker, P. Comte, P. Péchy, M. Grätzel, *J. Electrochem. Soc.* **153**, A2255 (2006)
28. G. Hodes, J. Manassen, D. Cahen, *J. Electrochem. Soc.* **127**, 544 (1980)
29. M. Peng, L.-L. Ma, Y.-G. Zhang, M. Tan, J.-B. Wang, Y. Yu, *Mater. Res. Bull.* **44**, 1834 (2009)
30. S. Gorer, G. Hodes, *J. Phys. Chem.* **98**, 5338 (1994)
31. O. Niiitsoo, S.K. Sarkar, C. Pejoux, S. Rühle, D. Cahen, G. Hodes, *J. Photochem. Photobiol. A* **181**, 306 (2006)
32. L. Han, N. Koide, Y. Chiba, T. Mitate, *Appl. Phys. Lett.* **84**, 2433 (2004)